

# Intrusion Detection for Industrial Control Systems: Evaluation Analysis and Adversarial Attacks

Giulio Zizzo<sup>\*†</sup>, Chris Hankin<sup>\*†</sup>, Sergio Maffei<sup>†</sup> and Kevin Jones<sup>‡</sup>  
<sup>\*</sup>Institute for Security Science and Technology (ISST), Imperial College London  
<sup>†</sup>Department of Computing, Imperial College London  
<sup>‡</sup>Airbus

g.zizzo17@imperial.ac.uk    c.hankin@imperial.ac.uk    sergio.maffei@imperial.ac.uk    kevin.jones@airbus.com

**Abstract**—Neural networks are increasingly used in security applications for intrusion detection on industrial control systems. In this work we examine two areas that must be considered for their effective use. Firstly, is their vulnerability to adversarial attacks when used in a time series setting. Secondly, is potential over-estimation of performance arising from data leakage artefacts.

To investigate these areas we implement a long short-term memory (LSTM) based intrusion detection system (IDS) which effectively detects cyber-physical attacks on a water treatment testbed representing a strong baseline IDS.

For investigating adversarial attacks we model two different white box attackers. The first attacker is able to manipulate sensor readings on a subset of the Secure Water Treatment (SWaT) system. By creating a stream of adversarial data the attacker is able to hide the cyber-physical attacks from the IDS. For the cyber-physical attacks which are detected by the IDS, the attacker required on average 2.48 out of 12 total sensors to be compromised for the cyber-physical attacks to be hidden from the IDS. The second attacker model we explore is an  $L_\infty$  bounded attacker who can send fake readings to the IDS, but to remain imperceptible, limits their perturbations to the smallest  $L_\infty$  value needed.

Additionally, we examine data leakage problems arising from tuning for  $F_1$  score on the whole SWaT attack set and propose a method to tune detection parameters that does not utilise any attack data. If attack after-effects are accounted for then our new parameter tuning method achieved an  $F_1$  score of  $0.811 \pm 0.0103$ .

**Index Terms**—machine learning, adversarial examples, security

## I. INTRODUCTION

Deep learning systems are known to be vulnerable to adversarial attacks at test time. By applying small changes to an input an attacker can cause a machine learning system to mis-classify with a high degree of success. There has been much work on both developing more powerful attacks [1] as well as defences [2]. However, the majority of adversarial machine learning research is focused on the image domain, with consideration of the different challenges that arise within other fields needed [3].

This phenomenon of adversarial examples becomes particularly pertinent when aiming to defend machine learn-

ing systems operating in a direct security domain. Machine learning, and specifically deep learning, systems frequently outperform other methods in detecting cyber attacks [4]–[7]. The use of deep learning systems can therefore be of great benefit, resulting in better defended cyber systems against non-adaptive attackers. Yet, adversarial example vulnerability means that adaptive attackers can pose an immediate risk.

Additionally, deep learning intrusion detection systems (IDS) frequently use many hyperparameters. With little attack data generally available, it is often difficult to form a distinct attack validation set. Therefore, care must be taken in interpreting  $F_1$  scores which use all of the available attack data to determine hyperparameter choices.

In this work we begin to determine a solution for these problems by considering how adversarial attacks can be mounted on time series based IDS and analyse evaluation methodology.

The contributions of this paper are as follows:

- We demonstrate the vulnerability of time series based intrusion detection to adversarial examples and are able to hide a range of real cyber-physical attacks from an IDS on an industrial control system (ICS).
- We discuss potential pitfalls with tuning and evaluating intrusion detection systems on the whole attack set of the Secure Water Treatment (SWaT) dataset and illustrate that unless the attack set is fully representative of all attacks that can occur in the ICS then the reported  $F_1$  scores will vary. We propose a baseline method which does not use the attack dataset in any manner to detect the various attacks.
- Finally, we present some benchmark results on a new dataset collected by iTrust in July 2019 showing that concept drift, even in a regular and relatively predictable system like SWaT, requires consideration.

## II. BACKGROUND

### A. Adversarial Examples

One of the most common occurrences of adversarial examples in literature is in conducting evasion attacks. In an evasion attack an attacker adds a perturbation to a datapoint  $x$  such that a neural network will output different classes for  $x$  and the perturbed datapoint  $\hat{x}$ . Commonly the distance,  $z = x - \hat{x}$ , is measured by one of three different norms:

- $L_\infty$  :  $\max|z_i|$ . This norm is the maximum change applied to any feature in the input.
- $L_0$  :  $\#\{i|z_i \neq 0\}$ . This represents the total number of features that can be altered. The selected features can be modified by any desired amount.
- $L_2$  :  $\sqrt{\sum_i z_i^2}$ . The  $L_2$  norm is the Euclidean distance between the original and perturbed datapoint.

There are a range of different attack crafting algorithms of differing speed and strength operating under different norms. For example, patch attacks perturb a complete section of an image, representing a  $L_0$  bound, and can be used to create adversarial stickers [8] and street signs [9] to fool image classifiers. In terms of  $L_\infty$  bounds one of the earliest attacks investigated, the Fast Gradient Sign Method (FGSM) [10], can quickly generate adversarial samples. It functions by perturbing each pixel in an image by fixed proportions to the sign of the gradient with respect to the desired class an attacker wishes to achieve. On the other end of the spectrum, in terms of attacker strength, the Carlini Wagner attack [1] optimises for data misclassification and simultaneously keeping the introduced perturbation as small as possible. This attack can operate under any of the three constraints.

Defences against adversarial examples are an active area of research using ideas from robust training [2], uncertainty [11], intermediate layer data representations [12], [13], or removing adversarial perturbations [14]. However, there is still no silver bullet to defending against all adversarial examples with techniques only working if the attacker is oblivious to their presence [15] or functioning effectively only against specific perturbation thresholds [2].

### B. Related Work for Intrusion Detection Systems

Machine learning can be used to detect anomalies in industrial control systems. Such detection systems often function in an autoregressive manner. Based on data at time steps  $x_0, \dots, x_t$  a prediction  $y_{t+1}$  is made for  $x_{t+1}$ . This prediction is compared to what is actually observed and the difference forms a residual,  $r_{t+1}$ . A detection function  $F_d$  is then employed to determine if an attack is occurring.  $F_d$  represents any operations which are computed on the residuals in order to generate an alert; examples include averaging, smoothing, and thresholding. The exact machine learning model and detection function vary across different works.

For example, long short-term memory (LSTM) networks were investigated in [16]–[18] for detecting cyber-physical attacks in the SWaT system with the best LSTM achieving a  $F_1$  score of 0.802. A different approach was taken in [19] which investigated the Gas Pipeline dataset [20] combining a filtering step followed by an LSTM prediction stage. If the observed data was not in the top 4 LSTM predictions then it was flagged as anomalous.

Many other architectures have been investigated. Among these, convolution neural networks [16] have shown to be able to give high  $F_1$  scores. Alternatively, autoencoders have been investigated [21], [22] as well as examinations into neural architecture search [23].

Recent work in [24] generated adversarial attacks for ICS when attacking an autoencoder IDS. In the white box case, the attacker queries the detector and substitutes the original data for sensor readings within normal sensor range. The potential perturbation applied in this way could be extremely large, as every sensor reading could be replaced from an arbitrary initial value during an attack, with a value that is within normal sensor range. Alternatively, generative methods can be used to create adversarial attacks such as in [25] where generative adversarial networks (GAN) were used to create adversarial data.

Concurrent work in [21] investigated adversarial attacks to target an autoencoder IDS. Unlike [24], the work in [21] modelled their attacker as not having control of the communications to the IDS independently of the programmable logic controller and so the adversarial data had to simultaneously fool the IDS and still fulfill the original cyber-physical attack. With this attack objective, even though the attacker had white box knowledge of the IDS and perfect knowledge of future values of the system, an effective adversarial attack was not found.

## III. INTRUSION DETECTION SYSTEM IMPLEMENTATION

To analyze the vulnerability of a time series based IDS to adversarial attacks we use the SWaT dataset [26] which is gathered on a water treatment ICS. There have been several detection systems proposed for the SWaT dataset [16], [18], [23], [27]. For this work, we train a LSTM [28] as our IDS as it represents a good literature baseline.

### A. Model

For the LSTM IDS we divide the data into sliding windows of 100 time steps. At each time step,  $t$ , the LSTM makes a prediction,  $y_{t+1}$ , for the next system state,  $x_{t+1}$ , based on the past datapoints  $x_1, \dots, x_t$  thus functioning in a sequence to sequence manner.

We used an LSTM with four layers, each with 512 hidden units and a dropout rate of 0.5 between layers. A set of dense layers takes the LSTM’s output at every time step and produces predictions for every feature.

At test time we take the difference between the predicted and observed values to form a series of residuals,  $r_1, \dots, r_t$ , for every predicted feature. We assume that the errors are normally distributed and so we compute means,  $\mu$ , and standard deviations,  $\sigma$ , of residuals on the validation data. The positive,  $R_t^p$ , and negative,  $R_t^n$ , residuals are then computed based on

$$R_t^p = \max(0, r_t - \mu - \sigma) \quad (1)$$

$$R_t^n = \min(0, r_t - \mu + \sigma). \quad (2)$$

Finally, we perform two cumulative sums over a sliding window containing 10 timesteps for both  $R_{1\dots t}^p$  and  $R_{1\dots t}^n$ . If the cumulative sum then exceeds a threshold across any of the predicted features then an anomaly is declared.

## B. Data Processing

For pre-processing we normalise continuous values to have zero mean, unit variance, and one-hot encoded categorical values. We remove features that have a constant value throughout the training and validation sets. Such data will not contribute to learning anything of significance and attacks on those features can be trivially detected by a straightforward check on the state of those actuators. We divide the data, 80% for training and 20% for validation.

Additionally, we saw that large parts of the test dataset which was marked as “normal” was fundamentally different from the training/validation data. Consider the sensor feature AIT201 as shown in Figure 1. We can see that the test data only remains in the range spanned by the training and validation data for a short period of time. In Figure 1 we removed the data marked as “Attack” and so all of the data shown represents normal behaviour. As the normal test data distribution is fundamentally different from the training data it is flagged as anomalous.

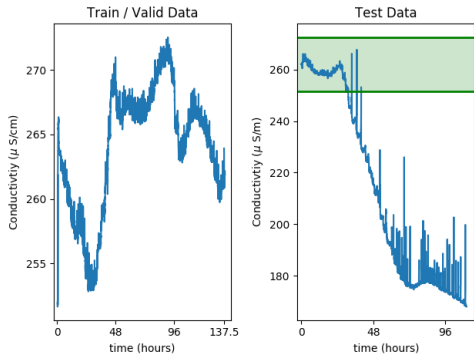


Fig. 1: Left: Training and validation data for the AIT201 sensor. Right: Test time data, the green area indicates the range spanned by the training and validation data.

Some works use test time statistics to normalise the test data and so sidestep the problem [17], [27] however that is generally poor practice. To address this issue we only use the features that relate to physical system properties in our IDS, i.e. flow and water level sensors as well as mechanical pumps and valves. These features did not experience such large deviations compared to many of the sensors relating to chemical properties of the water.

Concurrently with our work, the authors in [21] also noticed that there is a discrepancy between the test and training datasets for non-anomalous data. In their work they proposed the use of a modified Kolmogorov-Smirnov test to filter out such features.

Finally, although we feed into the IDS the sensor and actuator states, we only monitor the sensors for anomalies. This is a simplifying step which relates to the nature of crafting the adversarial attacks. As the optimisation algorithm we employ is only applicable to continuous values, restricting ourselves to monitoring only continuous data allows us more flexibility when choosing which sensor feature to compromise.

## C. IDS Results

Following the data pre-processing, we trained our LSTM and evaluated its performance on the SWaT test set. We fed the data in  $T$  second long sequential windows to the IDS. If in the most recent window an anomaly was detected we reset the LSTM’s internal state, otherwise we used the LSTM in a stateful manner between successive windows. This allowed for fewer cold starts to be experienced by the LSTM over the normal operation of the SWaT system. However, if an anomaly was encountered, we did not wish the anomaly to keep affecting the LSTM’s internal state after the attack has ended, hence our re-initialisations. The time window  $T$  is one of the hyperparameters determining the sensitivity of the detector. Shorter time windows are more prone to re-initialising the IDS as, at an extreme of  $T = 1$ , whenever an anomaly is triggered it will cause the LSTM to re-initialise. While at large values of  $T$  multiple anomalies would only cause a single re-initialisation. However, longer time windows can maintain attack after-effects for longer and so drive up the false positive rate. We did a small grid search of  $T = \{25, 50, 100, 150\}$  and 50 gave the best result.

We then tuned our detection thresholds by taking the cumulative sums of residuals of non-attack data. We computed the percentile scores and over a small grid search selected the 99.6th percentile score as the threshold for 6 sensors and 99.7th percentile score for the remaining 7 sensors. The results are in Table I and our LSTM based detection system achieves an  $F_1$  score of 0.8175 making it competitive with other literature baselines.

## IV. EVALUATION ANALYSIS

### A. Data Leakage Study

In a real world deployment, all of the methods cited in Table I, as well as ours, would most likely perform differently than the  $F_1$  scores would suggest. Currently, there is no distinct validation set with attacks, nor an established method of generating one. So all of the examined works, as well as our model, either perform hyperparameter tuning on the whole attack dataset to optimise for  $F_1$  performance or, in addition, use test time statistics. Effectively, this treats the attack set, which we test on, as a validation dataset. So, unless the attack set is fully descriptive of all the attacks that could occur, the  $F_1$  scores will vary when presented with completely new attacks.

We show experimental results investigating this effect. The attack dataset is split into a series of 50 second long windows, and from those windows we randomly select 20% to form a separate validation set and the rest we use for testing. We generate the thresholds based on the randomly selected 20%. As the validation set in this situation closely mirrors the remaining 80% of the test set we achieve an  $F_1$  score of 0.8166, which is comparable to tuning hyperparameters based on all of the attack set. In this evaluation, we used a stateless LSTM between datapoints as the data will not be continuous.

However, if a continuous 20% segment is chosen and hyperparameters are tuned on it then the results can vary significantly. We conduct the following procedure:

| Method            | $F_1$ score   |
|-------------------|---------------|
| MLP [23]          | 0.812         |
| SVM [17]          | 0.796         |
| DNN [17]          | 0.802         |
| MADGAN [27]       | 0.77          |
| Various [16]      | 0.609 - 0.775 |
| Autoencoders [21] | 0.873         |
| <b>Ours</b>       | <b>0.8175</b> |

TABLE I: Results for different literature benchmarks. For the work in [16] we report the performance of non ensemble methods from their result table.

- Divide the attack dataset into five equally sized continuous segments. Therefore, segment one contains the data in the first 0% - 20% of the attack dataset, segment two contains data in the 20% - 40% range, etc.
- Tune hyperparameters based on one of the segments.
- Report  $F_1$  performance on the the following combinations:
  - The remaining four test segments evaluated individually.
  - The remaining four test segments combined.
  - All five segments combined.

We can see from Table II that if the defender experiences novel attacks which they have not tuned on then the results are, as expected, worse than using all of the attack data. Furthermore, which segment the defender has access to causes itself variation across the  $F_1$  scores. Take as an example the final 80% - 100% of the data. On one hand, if the thresholds are chosen based on the first 20% of the data then an  $F_1$  score of 0.372 is achieved on it. However, if the thresholds are computed on itself, i.e. the final 80% - 100% of the data, then the  $F_1$  score becomes 0.642.

This presents an interesting area of future research, as novel attacks on which we have not tuned our hyperparameters can have unexpected properties which causes our  $F_1$  scores to vary significantly. As there is no guarantee that the attacks created in a attack dataset form a full representation of any attack that could occur, then  $F_1$  performance variations are to be expected.

To provide a baseline to address this we implemented a method to generate thresholds which does not rely on the attack data, test time statistics, or optimising for  $F_1$  score. Not relying on any attack data can be of practical importance to real world deployment. Unless a ICS operator is willing to generate a set of attacks to deploy a IDS, then all we have available is data of the system under normal operation.

We begin by taking our validation data, and we wish to account for normal system behaviour which deviates from its data. To that end we introduce noise by randomly selecting a time step from a 100 second window and replacing it with data drawn from a different 100 second window. We run the validation data through our model and select our thresholds based on the maximum and minimum cumulative residuals.

| Data Split (%)         | $F_1$ Score  |              |              |              |              |
|------------------------|--------------|--------------|--------------|--------------|--------------|
| 0 - 20                 | <b>0.526</b> | 0.469        | 0.400        | 0.479        | 0.461        |
| 20 - 40                | 0.186        | <b>0.251</b> | 0.188        | 0.200        | 0.189        |
| 40 - 60                | 0.897        | 0.879        | <b>0.941</b> | 0.895        | 0.889        |
| 60 - 80                | 0.313        | 0.404        | 0.320        | <b>0.591</b> | 0.308        |
| 80 - 100               | 0.372        | 0.552        | 0.586        | 0.627        | <b>0.642</b> |
| Test Segments Combined | 0.705        | 0.770        | 0.393        | 0.787        | 0.734        |
| All Segments Combined  | 0.694        | 0.737        | 0.782        | 0.776        | 0.727        |

TABLE II: Results for different validation / test splits on the SWaT attack dataset. Bold numbers under the  $F_1$  score indicates which split was used for the validation.

| Hyperparameter Generation Method | $F_1$ Raw Data    | $F_1$ Attack After-Effect Filtering |
|----------------------------------|-------------------|-------------------------------------|
| Original                         | 0.8175            | 0.836                               |
| Validation Only                  | $0.771 \pm 0.006$ | $0.811 \pm 0.0103$                  |

TABLE III:  $F_1$  scores depending on how the hyperparameters were computed and if the attack after-effects are considered false positives. We report values based on 10 different random noise additions when using only the validation data.

We set the time window size  $T$  of which to feed data into the IDS to be 100, equal to the original value of the sliding window used to train the IDS. We specifically do not tune the window to optimise for  $F_1$  as it will lead to data leakage from the attack set.

By running the test set data through the IDS we achieve a  $F_1$  score of  $0.771 \pm 0.006$ . However, it is now very important to define precisely when an attack’s effects stop. Many attacks have side effects which last far beyond when the attack is labelled as finishing. This will generally lower the performance of an IDS, as data which is anomalous, but not attack, is being flagged and counted as a false positive. However, if we know what the test data will be, then problem can be handled by tuning the detection thresholds and other hyperparameters to be less sensitive.

However, we have no such option as we are not using the attack dataset to tune our  $F_1$  metric. Thus, in Table III we additionally show results which do not consider anomalies which occur immediately after an attack concludes as a false positive. More precisely, we say that if there is a 100 second window without any anomalies after an attack is labelled as finishing then the attack’s secondary effects have also ended. Any anomalies from this point are considered normally while anomalies occurring before this condition is met are not considered false positives. This gives an  $F_1$  score of  $0.811 \pm 0.0103$ .

Using this procedure of considering attack after-effects on the original detector, when its hyperparameters were tuned in the conventional manner, caused the  $F_1$  score goes from 0.8175 to 0.836, a much more modest increase. This is, as mentioned previously, because we are considering the attack after-effects when hyperparameter tuning for  $F_1$  score.

## B. Concept Drift Performance

As a final analysis of our IDS we examine how well it performs on new data collected by the iTrust group in July 2019 [29]. As this is several years after the original data was collected we can immediately see differences in the ranges covered by sensor readings. To make the new dataset comparable to the original one we re-computed normalisation statistics. This was required to avoid all the data being considered anomalous by our detector through similar argument to that described in Figure 1. Thus, we compute new means and standard deviations based on the first 2 hours of system operation in the July 2019 dataset which does not contain attacks.

In addition, we re-labelled the dataset as the times provided to indicate when attacks begin and end do not match what we saw in the data. As an example, the first attack which involves spoofing the FIT401 value from 0.8 to 0.5. It is labelled as starting at 07:08:46 and finishing 07:10:31 however the FIT401 values are all 0.8 over that period. The spoofing actually occurs during 07:07:00 to 07:08:44. So that our results can be reproduced in Table IV we show when we labelled as attacks starting and stopping and the motivation for choosing that time.

After normalising the July 2019 dataset, we feed it though our model keeping all hyperparameters fixed. We found that our model failed to give any meaningful results on this newer dataset- virtually all of the data is flagged as anomalous. To begin obtaining better results we re-trained the LSTM on the first 7200 datapoints (corresponding to 2 hours of time) and used the next 1000 as the validation set, and then tune thresholds for  $F_1$  score. We achieved an  $F_1$  metric of 0.63. By determining the thresholds without using attack data in the manner described in section IV-A we achieve an  $F_1$  score of  $0.521 \pm 0.008$ .

As an additional benchmark we implemented the SVM anomaly detector model described in [17] and used the recommended hyperparameters. As described in the paper we normalised the training and test sets with their respective means and standard deviations. This achieved an F1 score of 0.8099 on the regular SWaT attack set. If we follow the more strict process of normalising the training and test sets with the training mean and standard deviation we achieve a score of 0.27709, very similar to the values reported in [17]. On the new July 2019 dataset we tried the best three hyperparameter combinations from [17] and the top performing SVM model achieved an  $F_1$  score of 0.529. These scores are significantly lower than what is achieved on the full SWaT dataset. We attribute this to two reasons. Firstly, the new dataset is small, thus turning the problem into one of transfer learning from the full SWaT dataset to the new smaller set of data. Re-training our model on the first two hours of data did help, but more sophisticated transfer learning techniques could boost performance further. The second potential reason for the disparity is the warping effect of attack number 23 in the original attack dataset. That attack is almost 10 hours in

duration containing over 63% of the total attack points, and is one of the easiest attacks to detect. This means even a simple detector can easily hit a recall of 0.732, even if no other attacks are detected. However, in the new dataset all of the attacks are over a more comparable time scale.

## V. ADVERSARIAL ATTACKS

Having defined and analysed the IDS we now turn our attention to an adaptive adversarial attacker. The attacker in our situation wishes to conduct a cyber-physical attack on an ICS. The cyber-physical attacks are represented by the attacks present in the SWaT dataset. An IDS can quickly detect these attacks, and so block the intended damage.

Thus, an attacker desires to conduct their attacks while remaining hidden from an IDS for the attack's entire duration. We analyse two different attacker models. Firstly, one in which the attacker is able to compromise  $k$  sensors in the system, and, by sending tampered data to the IDS aims to hide the dataset's cyber-physical attacks from the IDS. Effectively, the attacker is operating over an  $L_0$  constraint. This type of attack could represent a scenario when an attacker can compromise the communication between a sensor and the IDS. For example, in attack number 6 the water level as measured by the LIT301 sensor rapidly changes value. If the attacker can now control the data leaving the LIT301 sensor to the IDS, how can the data be altered in order to hide their attack? Simply reporting a constant fixed water level of LIT301's original measurement still triggers an alarm as the LIT301 values are not consistent with the rest of the system dynamics. It becomes even less intuitive if the adversary cannot send false sensor data on certain features. As an example, if the attacker turns on a pump to cause a cyber-physical attack and this pump state cannot be manipulated further, which of the sensors that trigger alerts should the attacker compromise, and what is the perturbation that should be added?

Secondly we consider the case where an attacker, rather than compromising individual sensors, is able to compromise a point on the network which enables them to modify all the sensor readings. This could be a man-in-the-middle attack between the supervisory control and data acquisition (SCADA) and IDS. With this capability, the attacker could change all the values to any desired state. However, what could be of interest is to perturb the data by the minimum amount needed as measured by an  $L_\infty$  norm. This could be advantageous for the attacker as if the attack requires little perturbation to hide it from the IDS, it will also be less perceivable by a human operator. Although the  $L_0$  attacks can fool the IDS, often the perturbations introduced can be visibly noticeable to an operator monitoring a human machine interface (HMI); an example can be seen later in Figures 3a and 3b. Conversely,  $L_\infty$  attacks can be harder to spot as shown in Figure 4b.

We now define the knowledge the attacker has of the SWaT system and then consider different attack algorithms under the two different norms.

| Attack Number | Used Attack Start / End | Offset from original labels | Motivation   |
|---------------|-------------------------|-----------------------------|--|
| 1             | 07:07:00 - 07:08:44     | -106s / -107s               | The FIT401 readings change from 0.8 to 0.5 over a different time window.   |
| 2             | 07:13:27 - 07:17:47     | -93s / -105s                | The LIT301 Readings change to 1024 over a different time window.   |
| 3             | 07:25:13 - 07:29:02     | -104s / -106s               | The P601 pump value changes from 1 to 2 over a different time window.  |
| 4             | 07:37:19 - 07:44:48.00  | -91s / -92s                 | As this attack involves two actuators being compromised at different times, we selected the actuator changes which kept the attack duration as close as possible to the original. Thus we declare the attack as occurring when both actuators are compromised. |
| 5             | 07:52:18 - 07:54:55.00  | -102s / -65s                | We defined the attack as starting when MV501 entered the value of 0, and finished when the MV501 value was again at 2.   |
| 6             | 08:01:06 - 08:15:07     | -110s / -111s               | The P301 valve changed from 2 to 1 over a different window.  |

TABLE IV: Attack times we used in our results for the July 2019 dataset and explanation as to why it was chosen.

### A. Attacker Knowledge

We model the attacker as having white box knowledge of the IDS and accurate knowledge of the physical system dynamics. Knowledge of the physical system dynamics has a large influence on the attacker strength, as if the attacker does not know how the system evolves in time, then all the attacker would be able to do is greedily optimise data as it arrives to minimise the residual at  $t+1$ . After the attacker has conducted the optimisation and sent the manipulated data to the IDS they will be unable to retroactively make changes to the data to aid them in keeping future attack data hidden.

However, if the attacker has an accurate model of the system then they can predict how it will evolve over the course of their attack. With this capability the attacker can now optimize the data with the aim of global stealth across all time steps. We represent this capability by assuming the attacker’s model of the physical system yields its ground truth, but cannot generate the appropriate sensor noise that will occur when a sensor takes a measurement. However, we only have access to the SWaT dataset which already has sensor noise present. Hence, to simulate this scenario we take the values in the SWaT dataset as the ground truth of the system and is what the attacker’s model of the physical system gives. This dataset,  $D_A$ , is therefore the knowledge the attacker has of how the system evolves. Then, we create a copy of the train and test datasets and add Gaussian noise to it. We select the level of noise based on the datasheets for the sensors used in the SWaT system. For the flow sensor data we add Gaussian noise with a standard deviation of 0.2% of the measured value. In the case of the water level data we add Gaussian noise with a standard deviation of 0.25% of the measured value or 6mm (whichever is greater). This set of data,  $D_d$ , is what the defender will see.

Rather than having a model of the system the alternative for the attacker in conducting their attacks is to perform them *a posteriori* i.e. once the attacker has received a series of sensor readings. However, that would be a stronger attacker model as they will not be concerned with sensor noise as they will have a perfect knowledge of the available data. This was the attacker model as studied in [21].

This requirement of having an accurate physical system model, or conducting the attacks *a posteriori*, is due to the fact that the detection system declares an anomaly conditioned on

all past datapoints. This requirement depends on the IDS being targeted. For example, in [24] a autoencoder was targeted which considers each data-point independently, so all the attacker needs to know is the data as it arrives sequentially.

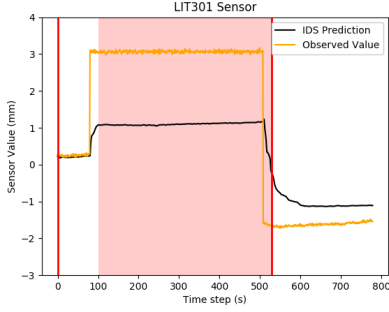
### B. Stronger Defender Model

We use the training portion of  $D_d$  to train the defender IDS using the model and detection function described in section III-A. For comparison to the results in Table I our LSTM trained with  $D_d$  achieved marginally higher results with an  $F_1$  score of 0.828. The slightly higher result may be because adding noise resulted in slightly better regularisation, or simply that our threshold grid search yielded better thresholds for the this model.

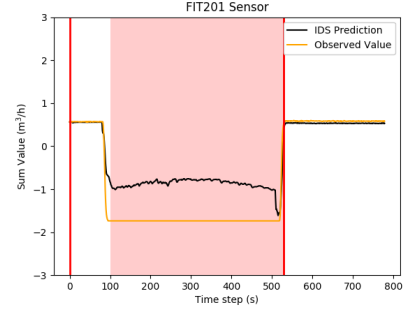
We now alter our detection thresholds to make the defender stronger against an adversarial attacker, as well as potentially more representative of a real world detection system.

The current detection thresholds were set by considering all of the data in the SWaT attack dataset. However, many of the cyber physical attacks have long term effects on the system which can require significant time to re-stabilize. This data, although anomalous, is not labelled as an attack and so would contribute to the false positive rate. Hence, this results in detection thresholds being artificially raised. So, rather than devise a system that works effectively across all the dataset sequentially we tighten our thresholds based on data that is clear of any secondary effects that occur after an attack has finished.

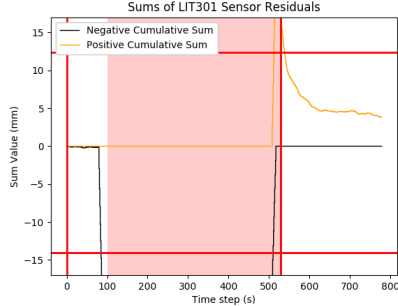
We divide the SWaT attack dataset into sequences of data that is “clean” of secondary effects by extracting sequences of data whose start point is 600 seconds after an attack finishes, and the end point is 100 seconds before an attack begins. Empirically, 600 seconds after an attack finished was sufficiently long (barring one case) to not observe negative attack after-effects. Defining the end point of a “clean” data sequence to occur 100 seconds before an attack started was done because in some cases the attack seemingly began prior to attack label indicating an attack was in progress. As an example, consider the first cyber-physical attack in the dataset. It is defined by opening the MV101 valve when it should be closed. The attack is labelled as beginning at time 10:29:14, but the MV101 valve changes state at 10:28:50, 28 seconds before the attack is labelled as starting. Another example



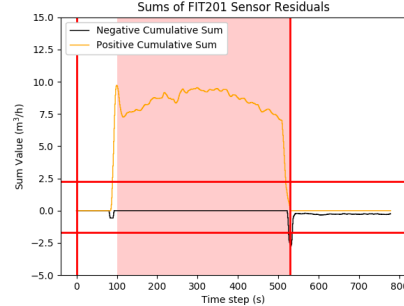
(a) The original readings for sensor LIT301.



(b) The original readings for sensor FIT201.



(c) The residuals accumulate to trigger a large alert on the LIT301 sensor when no adversarial methods are used.



(d) The residuals accumulate to trigger an alert on the FIT201 sensor when no adversarial methods are used..

Fig. 2: We can see here the results for the LIT301 (left plots) and FIT201 sensor (right plots) for attack number 6 when there is no compromise in the system. Red vertical lines indicate when the attacker began and ended their optimisation and the shaded area indicates when the cyber-physical attack was in progress. Horizontal red lines show detection thresholds.

can be seen in Figure 2a with attack number 6 where the LIT301 sensor began reporting extremely high water level readings before the attack labels indicated that an attack was in progress. Finally, any resulting sequences of clean data shorter than 1500 seconds are discarded.

As mentioned previously, we have an exception to our heuristic of selecting clean sequences 600 seconds after an attack finishes and 100 seconds before an attack starts. This exception is the set of non-attack values between attacks 23 and 24. The system takes almost all of the duration between those two attacks to return to normal operation and so we do not use that fragment of data.

To determine our attack detection capability we extract out from the test set time windows starting 400 seconds before an attack starts and finishing when the attack ends. For attacks which have a smaller window than 400 seconds between each other we use the largest of either 100 or 25 second windows.

We run these sequences of data through our model and tune the thresholds using the same procedure as in section III-C. With this setup we obtain a recall of 0.821 due to the tighter decision boundaries giving the attacker a more challenging target. In terms of recall, which is a good measure of how difficult a target the IDS will be for an attacker, this places us close to the strongest literature results for dedicated defence papers (0.821 vs 0.827 [21]). Note, that although we achieve an  $F_1$  score of 0.872, the  $F_1$  score is *not* comparable to the

results in Table I as we are computing the scores by removing sections of data in the procedure described earlier to compute and evaluate the thresholds.

## VI. ATTACK ALGORITHMS

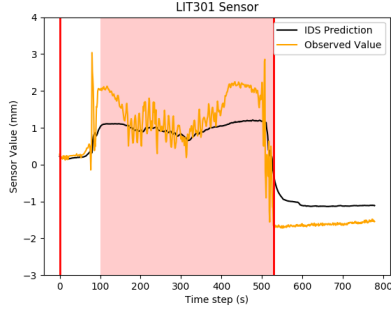
### A. $L_0$ Optimisation Attack

In the optimisation attack the attacker sends adversarial data on the compromised sensors to the IDS to hide the cyber physical attacks across all monitored sensors. The IDS generates residuals  $r_1 \dots r_N$  which are passed through a detection function  $F_d$  which outputs zero if no attack is detected or  $\eta_t$ , which is the magnitude by which an alert is generated. The attackers goal is thus to minimise the detection loss  $L_D$ :

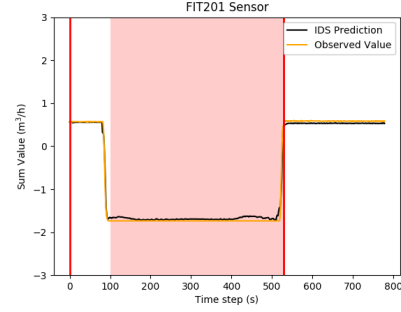
$$L_D = \sum_{t=0}^{t=N} F_d(r_1 \dots r_N). \quad (3)$$

Although the attacker is able to alter the data on the compromised sensor they do not have complete freedom as the compromised sensor itself is monitored. Specifically, the adversarial datapoint  $\hat{x}_t$  will cause the IDS to make a prediction  $y_{t+1}$  which must be close to the adversarial datapoint  $\hat{x}_{t+1}$ . However,  $\hat{x}_{t+1}$  is changing every iteration step as it is itself being updated. This creates a dynamic that is not usually present in static data like images, as here the optimisation target for the attacker changes from iteration step to iteration step.

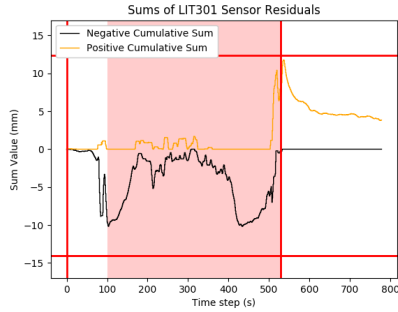




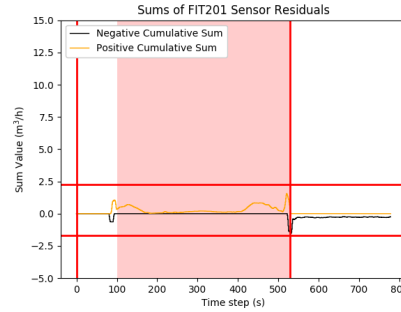
(a) The LIT301 sensor readings when an adversary optimises to reduce the residuals to below detection across all sensors.



(b) The FIT201 sensor readings when an adversarial attacker optimises to reduce the residuals to below detection



(c) The LIT301 residual sums resulting from the adversarial attack.



(d) The FIT201 residual sums resulting from the adversarial attack.

Fig. 3: Following from the plots in Figs. 2a - 2d here we see how an adversary manipulates LIT301 data to evade detection.

This presented a challenging optimisation problem and we used the BFGS algorithm as our optimiser [30]. Weaker first order optimisation methods (gradient decent, Adam, etc) did not find satisfactory solutions. This presents a deviation from image based adversarial attacks as in the image domain simple adversarial attacks, for example FGSM [10], are able to achieve high success rates against undefended neural networks.

### B. $L_0$ Prediction Based Attack

This attack exploits the autoregressive nature of the LSTM IDS and functions by feeding the LSTM's predictions back to itself as though it was real sensor data. More explicitly, if the attacker has the neural network model, then at time  $t$  they can compute the IDS's predictions for the next time step  $y_{t+1}$ . Then, at  $t + 1$ , on the sensors the attacker has compromised, rather than sending the real data,  $x_{t+1}$ , they send  $y_{t+1}$  to the IDS- i.e at every time step they perfectly match the data they send to the IDS with its own prediction for the system state.

This attack method does not make any active attempts to reduce detection on additional monitored sensors and so hiding attacks which have been detected on more sensors that the attacker has compromised is not guaranteed to succeed.

However this method does have advantages for the attacker in that the knowledge they need of the target system is lower. The detection function,  $F_d$ , and a model of the physical system

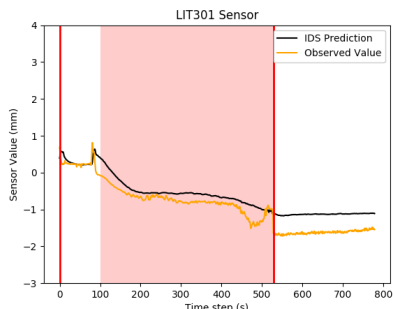
dynamics are only needed here to identify which sensors to compromise, but not to actually run the attack. In other words, if the attacker already has a set of compromised sensors then they can run this attack only needing the model of the LSTM. Conversely, the other attacks described will always need additional knowledge (such as  $F_d$  and  $D_a$ ) to compute the required perturbations.

This method can be combined with the  $L_0$  optimization attack by first running the prediction attack which provides an initialisation closer to the final goal. In our experiments this often led to better results when compared with starting the optimisation attack from the original data, particularly when a high number of features needed to be compromised to fully hide an attack. Additionally, this attack method generates sensor sequences which are often more plausible to a human viewer, thereby making the attack more stealthy with the same level of compromise as a pure optimisation approach. An example can be seen in Figure 4b.

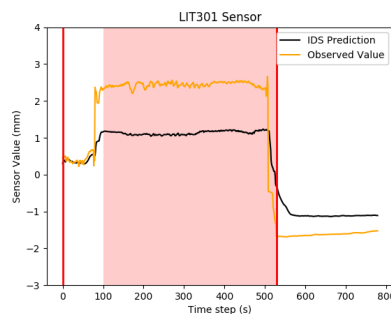
### C. $L_\infty$ Optimisation Attack

In this attacker model we assumed that the attacker has compromised a point in the network in which they are able to tamper with all of the continuous sensor readings. We examined an attacker's capability in hiding attacks at varying levels of an  $L_\infty$  bound. If at low levels of perturbation the cyber-physical attacks can be hidden it makes them hard to be





(a) Adversarial data when running the  $L_0$  prediction and  $L_0$  optimisation attack for attack number 6. Compared to Fig. 3a the adversarial data is much smoother and more plausible.



(b) Adversarial data when running the  $L_\infty$  attack for attack number 6. Compared to Fig. 3a the adversarial data is much smoother and more plausible.

Fig. 4: Plots showing data generated by the  $L_0$  prediction and  $L_\infty$  attacks.

spotted by other means, for example a human viewing a HMI monitor, compared to an  $L_0$  optimisation attack.

In this situation we are still constrained by the LSTM’s monitoring of the continuous features as described in section VI-A. However, unknown sensor noise will not affect the attacker as they are able to perturb all of the sensor data.

## VII. ADVERSARIAL ATTACK RESULTS

For every attack in the dataset we begin optimising either 400, 100, or 25 seconds before the cyber-physical attack begins to aid in hiding the initial portion of the attack. The largest time window was chosen which did not contain a false positive and did not begin during a previous attack.

### A. $L_0$ Constrained Attacks

For the  $L_0$  constrained attacker we need to determine which features the attacker should compromise. Hence, we select features based on the detection loss  $L_D$  computed on the dataset  $D_a$  which the attacker controls. Note, from Section V-A that the dataset  $D_a$  differs from the dataset which the defender will see  $D_d$  due to the addition of extra sensor noise.

We then run the  $L_0$  optimisation attack and if the detection loss is greater than zero we increase the level of compromise by including the feature with the highest level of detection loss post-optimisation. This continues iteratively until, based on the attacker dataset  $D_a$ , the attacker has zero detection loss. For each cyber-physical attack we explore three strategies:

- Use only the  $L_0$  prediction attack.
- Use only the  $L_0$  optimisation attack.
- Use the  $L_0$  prediction attack and then apply the  $L_0$  optimisation attack.

Once zero detection loss is achieved on  $D_a$  we check for pruning of the compromised features. As the compromised feature  $k_i$  was selected conditioned on the compromised features  $k_0, \dots, k_{i-1}$  the effect of more recent compromised features  $k_{i+1}, \dots, k_{i+n}$  may make the compromise of feature  $k_i$  unneeded. Thus, we iterate backwards removing compromised features beginning at  $k_{i+n-1}$  and checking that zero detection

loss is still achieved. If it is achieved we remove  $k_i$  from the features needing compromise.

The manipulated data then replaces the appropriate features in the defender’s dataset  $D_d$  and it is run through the IDS. If the attack achieves zero detection loss then the attack was successful. However, due to unknown sensor noise in uncompromised features the attack may fail. To account for this unknown noise the attacker optimises to 90% of the threshold values. The principle behind this is that if an attack can be optimised to lie below 90% of the real detection threshold, then even if there is some additional noise, it will not drive the cumulative residuals above the full detection threshold. This heuristic worked for all bar one case: in attack number 26 the detection loss was zero when using  $D_a$  but, when substituting the appropriate data into  $D_d$  there was a detection loss of 0.0497 down from an original detection loss of 356.79.

The full set of results is shown in Table V in which we show the minimum compromise needed to generate an adversarial attack. If different attack algorithms resulted in the same level of compromise we state the best algorithm to use according to the following rankings:

- 1)  $L_0$  Prediction attack: this attack requires only the LSTM model to function and generates plausible looking sensor measurements. Additionally, it can be run without  $D_a$  and  $F_d$  if a set of compromised sensors has already been identified.
- 2)  $L_0$  Prediction followed by  $L_0$  Optimisation: here we require a high level of knowledge, but still maintain plausible sensor measurements.
- 3)  $L_0$  Optimisation attack: requires a high level of knowledge, and a human may spot that the sensor readings are not realistic. This may not matter if the attack is quick, or if a human operator is not part of the defensive structure of the targeted plant.

On average 2.48 compromised sensors are required to hide a cyber-physical attack out of 12 total sensors. Broadly, the more features over which an attack is detected the more features

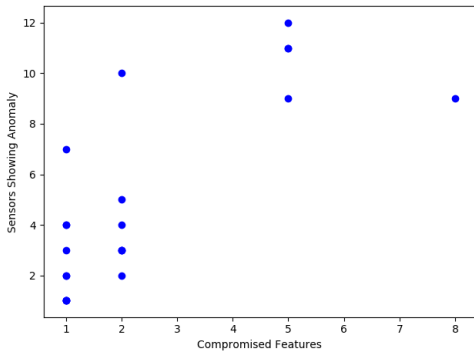


Fig. 5: The number of monitored features which triggered an alert against the level of compromise needed to hide the attack.

need compromising: on average attacks which were detected on 6 or more sensors required 4.5 sensors to be compromised while attacks which were detected on less than 6 sensors required 1.4 compromised sensors. From Figure 5 we can see that the number of sensors which detected an attack was occurring provides an indication to the number of features requiring compromise, and so can give the attacker an estimate of how much system compromise will be required.

To gain a better feel for how the attack modifies the data we show a portion of attack number 6 in Figures 2a - 3d. We show two sensors which trigger an alert in response to the attack. Figures 2a and 2b show how the observed readings for sensors LIT301 and FIT201 differ from the predicted values generating large residuals shown in Figures 2c and 2d which go above the detection thresholds.

The attacker is then able to compromise the LIT301 sensor and optimises to keep the residuals hidden across all of the sensors which triggered an anomaly (LIT301, LIT101, FIT201, FIT504). In Figure 3a we see what the observed values become for the LIT301 sensor to achieve this. Then, in Figure 3b we see the effect this has had on the predicted values for FIT201 and they now match very closely to the observed values. Finally, in the last two Figures 3c and 3d we see that the residuals have been reduced to as to not trigger an alert.

### B. $L_\infty$ Constrained Attacks

For the  $L_\infty$  constrained attack we begin to iteratively increase the perturbation level from  $\epsilon = 0.025$  until the attack is hidden. The range of perturbations needed for different attacks varied significantly, some attacks such as attack number 3 were immediately hidden with a perturbation of 0.025 while others, such as attack number 8, required an enormous levels of perturbation.

We show in Figure 6 the level of perturbation required against the detection loss of the various attacks. We can see that as the level of detection increases the higher the required level of perturbation. In effect this means certain attacks require such a high level of perturbation that the attacker can do as they wish. However, there are a set of attacks which can

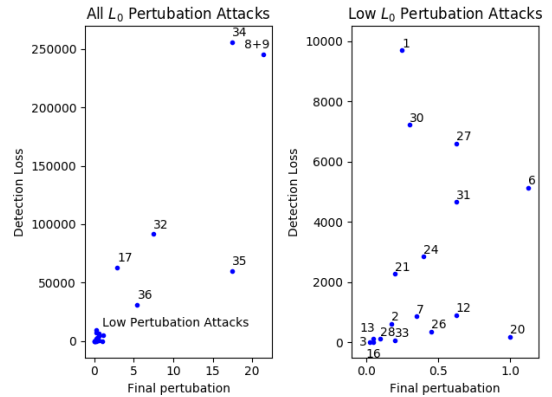


Fig. 6: Plots examining the detection loss against the  $L_\infty$  bound required to hide the attack. For a subset of attacks the amount of perturbation required is extremely large. On the right we can see a zoomed in plot of the attacks that require lower levels of perturbation. Attacks which occur back to back in the attack set are considered together (attacks 8 + 9 and 22 + 23). See Table V for more details. Not shown is attack 22 + 23 due to its loss of over  $4 \times 10^6$  skewing the axis. It required a perturbation of 10.0.

be hidden with a relatively low amount of perturbation shown on the right of Figure 6.

## VIII. CONCLUSION

We have presented a method for generating adversarial attacks on time series IDS. Although intrusion detection systems can be fooled they require a higher degree of perturbation and stronger optimisation strategies in comparison to adversarial samples in the image domain. For future work we will examine how to extend our attack algorithms to deal with mixtures of discrete and continuous data.

Additionally, we discussed the effects of using the whole attack set to generate hyperparameter choices when optimising for the  $F_1$  score. If the attack set is fully descriptive of all potential attacks that occur then there is no problem with this practice. If not then our  $F_1$  performance can vary significantly. As we have no guarantee that our datasets are fully descriptive in terms of attacks examining how we can make robust detectors using less ICS attack data is an interesting avenue for future work.

Finally, we presented results on examining the effects of concept drift in the SWaT system with the newly released July 2019 dataset. Our detector and a implementation of a simple literature baseline performed worse compared to the original SWaT attack set. This indicates an additional line of research where better methods for handling concept drift need to be investigated for ICS.

TABLE V: Complete Table of Results. Attack pairs 8 / 9 and 22 / 23 occur back to back in the attack dataset with no time between them. We state the results for detection when considering the attacks separately and together (8 + 9 and 22 + 23). For our adversary we consider the back to back attacks together forming as a single longer attack as it would be unrealistic for an attacker to begin optimising to hide an attack when the system was already in an unstable state from a previous attack which was detected immediately beforehand. Notes: for attack 22 + 23 we used the L-BFGS-B algorithm rather than BFGS due to computational constraints.

| Attack Number | Num of Channels with Detection | Num of Compromised Channels to Hide Attack | Adversarial Method Used   |
|---------------|--------------------------------|--|---|
| 1             | 2                              | 1  | $L_0$ Prediction  |
| 2             | 1                              | 1  | $L_0$ Prediction  |
| 3             | 1                              | 1  | $L_0$ Prediction  |
| 4             | NA                             | NA   | NA  |
| 5             | NA                             | NA   | NA  |
| 6             | 4                              | 1  | Initialised with $L_0$ Prediction, followed by $L_0$ Optimisation |
| 7             | 9                              | 3  | Initialised with $L_0$ Prediction, followed by $L_0$ Optimisation |
| 8 + 9         | 11                             | 5  | Initialised with $L_0$ Prediction, followed by $L_0$ Optimisation |
| 8             | 10                             | NA   | NA  |
| 9             | 11                             | NA   | NA  |
| 10            | 0                              | NA   | NA  |
| 11            | 0                              | NA   | NA  |
| 12            | 2                              | 2  | $L_0$ Prediction  |
| 13            | 3                              | 2  | $L_0$ Optimisation  |
| 14            | 0                              | NA   | NA  |
| 15            | 0                              | NA   | NA  |
| 16            | 1                              | 1  | $L_0$ Prediction  |
| 17            | 11                             | 5  | Initialised with $L_0$ Prediction, followed by $L_0$ Optimisation |
| 18            | 0                              | NA   | NA  |
| 19            | 0                              | NA   | NA  |
| 20            | 3                              | 1  | $L_0$ Prediction  |
| 21            | 4                              | 2  | $L_0$ Prediction  |
| 22 + 23       | 12                             | 10   | Initialised with $L_0$ Prediction, followed by $L_0$ Optimisation |
| 22            | 8                              | NA   | NA  |
| 23            | 11                             | NA   | NA  |
| 24            | 0                              | NA   | NA  |
| 25            | 3                              | 2  | $L_0$ Prediction  |
| 26            | 5                              | NA   | Attack Fails due to sensor noise                                  |
| 27            | 4                              | 1  | $L_0$ Optimisation  |
| 28            | 3                              | 2  | Initialised with $L_0$ Prediction, followed by $L_0$ Optimisation |
| 29            | 0                              | NA   | NA  |
| 30            | 1                              | 1  | $L_0$ Prediction  |
| 31            | 5                              | 2  | $L_0$ Optimisation  |
| 32            | 12                             | 5  | Initialised with $L_0$ Prediction, followed by $L_0$ Optimisation |
| 33            | 2                              | 1  | $L_0$ Optimisation  |
| 34            | 10                             | 2  | Initialised with $L_0$ Prediction, followed by $L_0$ Optimisation |
| 35            | 9                              | 5  | Initialised with $L_0$ Prediction, followed by $L_0$ Optimisation |
| 36            | 7                              | 1  | $L_0$ Prediction  |

## REFERENCES

- [1] Nicholas Carlini and David Wagner. Towards evaluating the robustness of neural networks. In *2017 IEEE Symposium on Security and Privacy (SP)*, pages 39–57. IEEE, 2017.
- [2] Aleksander Madry, Aleksandar Makelov, Ludwig Schmidt, Dimitris Tsipras, and Adrian Vladu. Towards deep learning models resistant to adversarial attacks. *arXiv preprint arXiv:1706.06083*, 2017.
- [3] Nicholas Carlini and David Wagner. Audio adversarial examples: Targeted attacks on speech-to-text. *arXiv preprint arXiv:1801.01944*, 2018.
- [4] Gyuwan Kim, Hayoon Yi, Jangho Lee, Yunheung Paek, and Sungroh Yoon. Lstm-based system-call language modeling and robust ensemble method for designing host-based intrusion detection systems. *arXiv preprint arXiv:1611.01726*, 2016.
- [5] Matilda Rhode, Pete Burnap, and Kevin Jones. Early stage malware prediction using recurrent neural networks. *arXiv preprint arXiv:1708.03513*, 2017.
- [6] Kathrin Grosse, Nicolas Papernot, Praveen Manoharan, Michael Backes, and Patrick McDaniel. Adversarial perturbations against deep neural networks for malware classification. *arXiv preprint arXiv:1606.04435*, 2016.
- [7] Ahmad Javaid, Quamar Niyaz, Weiqing Sun, and Mansoor Alam. A deep learning approach for network intrusion detection system. In *Proceedings of the 9th EAI International Conference on Bio-inspired Information and Communications Technologies (formerly BIONETICS)*, pages 21–26. ICST (Institute for Computer Sciences, Social-Informatics and Telecommunications Engineering), 2016.
- [8] Tom B Brown, Dandelion Mané, Aurko Roy, Martín Abadi, and Justin Gilmer. Adversarial patch. *arXiv preprint arXiv:1712.09665*, 2017.
- [9] Kevin Eykholt, Ivan Evtimov, Earlene Fernandes, Bo Li, Amir Rahmati, Chaowei Xiao, Atul Prakash, Tadayoshi Kohno, and Dawn Song. Robust physical-world attacks on deep learning models. *arXiv preprint arXiv:1707.08945*, 2017.
- [10] Christian Szegedy, Wojciech Zaremba, Ilya Sutskever, Joan Bruna, Dumitru Erhan, Ian Goodfellow, and Rob Fergus. Intriguing properties of neural networks. *arXiv preprint arXiv:1312.6199*, 2013.
- [11] Reuben Feinman, Ryan R Curtin, Saurabh Shintre, and Andrew B Gardner. Detecting adversarial samples from artifacts. *arXiv preprint arXiv:1703.00410*, 2017.
- [12] Nicolas Papernot and Patrick McDaniel. Deep k-nearest neighbors: Towards confident, interpretable and robust deep learning. *arXiv preprint arXiv:1803.04765*, 2018.
- [13] Giulio Zizzo, Chris Hankin, Sergio Maffei, and Kevin Jones. Deep latent defence. *arXiv preprint arXiv:1910.03916*, 2019.
- [14] Weilin Xu, David Evans, and Yanjun Qi. Feature squeezing: Detecting adversarial examples in deep neural networks. *arXiv preprint arXiv:1704.01155*, 2017.
- [15] Nicolas Papernot, Patrick McDaniel, Xi Wu, Somesh Jha, and Ananthram Swami. Distillation as a defense to adversarial perturbations against deep neural networks. In *Security and Privacy (SP), 2016 IEEE Symposium on*, pages 582–597. IEEE, 2016.
- [16] Moshe Kravchik and Asaf Shabtai. Detecting cyber attacks in industrial control systems using convolutional neural networks. In *Proceedings of the 2018 Workshop on Cyber-Physical Systems Security and Privacy*, pages 72–83. ACM, 2018.
- [17] Jun Inoue, Yoriyuki Yamagata, Yuqi Chen, Christopher M Poskitt, and Jun Sun. Anomaly detection for a water treatment system using unsupervised machine learning. *arXiv preprint arXiv:1709.05342*, 2017.
- [18] Jonathan Goh, Sridhar Adepu, Marcus Tan, and Zi Shan Lee. Anomaly detection in cyber physical systems using recurrent neural networks. In *High Assurance Systems Engineering (HASE), 2017 IEEE 18th International Symposium on*, pages 140–145. IEEE, Jan 2017.
- [19] C. Feng, T. Li, and D. Chana. Multi-level anomaly detection in industrial control systems via package signatures and lstm networks. In *2017 47th Annual IEEE/IFIP International Conference on Dependable Systems and Networks (DSN)*, pages 261–272, June 2017.
- [20] Thomas H Morris, Zach Thornton, and Ian Turnipseed. Industrial control system simulation and data logging for intrusion detection system research. *7th Annual Southeastern Cyber Security Summit*, 2015.
- [21] Moshe Kravchik and Asaf Shabtai. Efficient cyber attacks detection in industrial control systems using lightweight neural networks. *arXiv preprint arXiv:1907.01216*, 2019.
- [22] Riccardo Taormina and Stefano Galelli. Deep-learning approach to the detection and localization of cyber-physical attacks on water distribution systems. *Journal of Water Resources Planning and Management*, 144(10):04018065, 2018.
- [23] Dmitry Shalyga, Pavel Filonov, and Andrey Lavrentyev. Anomaly detection for water treatment system based on neural network with automatic architecture optimization. *arXiv preprint arXiv:1807.07282*, 2018.
- [24] Alessandro Erba, Riccardo Taormina, Stefano Galelli, Marcello Pogliani, Michele Carminati, Stefano Zanero, and Nils Ole Tippenhauer. Real-time evasion attacks with physical constraints on deep learning-based anomaly detectors in industrial control systems. *arXiv preprint arXiv:1907.07487*, 2019.
- [25] Cheng Feng, Tingting Li, Zhanxing Zhu, and Deepch Chana. A deep learning-based framework for conducting stealthy attacks in industrial control systems. *arXiv preprint arXiv:1709.06397*, 2017.
- [26] Jonathan Goh, Sridhar Adepu, Khurum Nazir Junejo, and Aditya Mathur. A dataset to support research in the design of secure water treatment systems. In Grigore Havarneanu, Roberto Setola, Hypatia Nassopoulos, and Stephen Wolthusen, editors, *Critical Information Infrastructures Security*, pages 88–99. Cham, 2017. Springer International Publishing.
- [27] Dan Li, Dacheng Chen, Lei Shi, Baihong Jin, Jonathan Goh, and See-Kiong Ng. Mad-gan: Multivariate anomaly detection for time series data with generative adversarial networks. *arXiv preprint arXiv:1901.04997*, 2019.
- [28] F.A. Gers, J. Schmidhuber, and F. Cummins. Learning to forget: continual prediction with lstm. *IET Conference Proceedings*, pages 850–855(5), January 1999.
- [29] itrust dataset characteristics. [https://itrust.sutd.edu.sg/itrust-labs\\_datasets/dataset\\_info/](https://itrust.sutd.edu.sg/itrust-labs_datasets/dataset_info/). Accessed: 2019-10-1.
- [30] R. Fletcher. *Practical Methods of Optimization; (2Nd Ed.)*. Wiley-Interscience, New York, NY, USA, 1987.